ISSN 0915-633X

NATIONAL INSTITUTE FOR FUSION SCIENCE

Effects of High Z Probe on Plasma Behavior in HT-6M Tokamak

J. Li, X. Gong, L. Luo, F.X. Yin, N. Noda, B. Wan, W. Xu, X. Gao, F. Yin, J.G. Jiang, Z. Wu., J.Y. Zhao, M. Wu, S. Liu and Y. Han

(Received - Aug. 30, 1996)

NIFS-451 Sep. 1996

RESEARCH REPORT
NIFS Series

NAGOYA, JAPAN

Effects of High Z Probe on Plasma Behavior in HT-6M Tokamak

J. Li, X. Gong, L. Luo, F. X. Yin, N. Noda[1], B. Wan, W. Xu, X. Gao, F. Yin, J. G. Jiang, Z. Wu., J. Y. Zhao, M. Wu, S. Liu, Y. Han

Institute of Plasma Physics, Academia Sinica, Hefei, 230031, P. R. China

[1] National Institute for Fusiion Science, Nagoya 464-01, Japan

---

A revised manuscript of a contributed paper orally presented in 12th International Conference on Plasma Surface Interactions in Controlled Fusion Devices held at Saint Raphael from May 20 to 24, 1996. To be published in J. Nucl. Materials.

Abstract

Molybdenum and tungsten probes have been tested in HT-6M tokamak under various discharge conditions aiming to find out the conditions in which high Z PFC can be used without serious degradation of core plasma performance. In normal OH discharges, the degradation of core plasma performance was found only when the probe was inserted beyond 3.0 cm inside the last closed flux surface (LCFS). The plasma performance did not change with positive biasing to the probe, whereas central T_e degraded during negative biasing of -100 V. The insertion of the Mo probe to 1.5 cm inside the LCFS made a change in the threshold power of the L-H transition in EOH discharges. These results suggest a certain operation range of the H-mode in the EOH discharge with the Mo probe in HT-6M.

Key Words: high Z wall material, biasing, impurity source, improved confinement mode, erosion & particle deposition, HT-6M

1. Introduction

In this decade, the major emphasis in fusion research has been put on achievement of reactor relevant high plasma parameters. This target has been cleared with low Z wall such as carbon, beryllium or boron. Some problems are pointed out for low Z materials as the plasma facing components (PFC) in future DT, long burn machines, namely, high erosion rate, large tritium inventory and impacts of DT neutron irradiation damages [1, 2]. High Z materials are possible alternate for the PFC because of their erosion resistance and good thermal conductivity.

In TEXTOR, molybdenum or tungsten test limiters have been used to evaluate the impact of high Z PFC, and some interesting results have been reported [3 - 5]. A flat profile of electron temperature T_e has been observed due to peaked radiation loss by high Z impurities in high density ohmic heated (OH) discharges. However, no T_e degradation has been seen in NBI and ICRF heated discharges. In ASDEX-Upgrade, high Z impurity behavior has been investigated by using laser blow-off technique [6] and recently with a toroidal tungsten divertor [7]. The major plasma facing components in Alcator C-Mod are molybdenum tiles [8]. No serious effects of high Z PFC has been found with OH and ICRF discharges in ASDEX-Upgrade and Alcator C-Mod.

Although these results are encouraging for the possibility of high Z PFC in future, systematic investigations are required to get comprehensive understanding on the behavior of plasmas with the high Z PFC. The existing data base is very limited compared with those for low Z PFC. There is no result given by a small size tokamak. A lot of work is left before approaching to the goal of this study, that is, in which condition the high Z PFC is available without any serious degradation of core plasma performance. In order to meet this requirement, a series of experiments has been started in HT-6M by using a movable Mo or W probe, of which results with the Mo probe are presented in this paper.

A small Mo or W test probe was inserted inside the last closed flux surface (LCFS) of HT-6M plasmas. The method was similar to the TEXTOR experiments on high Z limiters. New aspects different from TEXTOR were application of negative or positive bias to the test plobe, and investigation of impacts of the probe upon L-H transition behavior. The biasing experiment was once applied to an aluminum target in DIVA tokamak, with which the dominant release mechanism of the limiter materials was identified as the ion sputtering for the first time [9]. The molybdenum probe was also tested with an improved confinement discharges of Edge Ohmic Heating (EOH) and Lower Hybrid Current Drive (LHCD). Some preliminary results are presented for the first series of this experimental study in this paper.

2. Experimental setup

HT-6M is a small air-core tokamak with the following parameters: major radius R = 65 cm, minor radius a = 20 cm, magnetic field strength B_T = 0.7 - 1.3 T, plasma current I_p = 50 - 90 kA, central electron temperature T_{e0} = 500 - 760 eV, ion temperature T_i = 200 - 300 eV, line averaged

electron density , n_e = 0.5 - 4.0 x 10^{19} /m^3. During this experiment, the probe was inserted to the plasma through a port hole located 30 degrees above the mid plane in poloidal direction. The head of the probe could be replaced without exposing the torus to the air. Density profile $n_e(r)$ was measured with a 7-channels HCN interferometer, temperature profile $T_e(r)$ with a Si-Li detector system, radiation power P_{rad} with a bolometer system, edge electron temperature profile $T_e(r)$ by Langmuir probes. Visible line emissions of H_α, CIII, OII, MoI (319.8 and 386.4 nm) were monitored at the probe head by a CCD camera with different sets of interference filters. Effective Z value Z_{eff} was monitored with a Z-meter.

The radius of the main limiter was fixed at 21.5 cm, and the last closed flux surface (LCFS) was determined as 19.5 cm by a movable half-turn limiter made of stainless steel. The Mo or W probe had cylindrical shape of 4 cm in diameter. Its length was 3.5 or 6.0 cm. The head was electrically insulated from the vacuum chamber.

3. Experimental results

3.1. Ohmic discharges without biasing

For normal ohmic heated (OH) discharge, no degradation of core plasma performance was found when the probe was inserted less than 2.5 cm inside the LCFS. In Fig. 1, parameters at a flat-top phase (at 15 ms from the start) of the discharges are plotted as a function of the probe location. Plasma current I_p was 66 kA, field strength B_T 1.0 T, central electron temperature T_{e0} 600 - 700 eV, line averaged density n_e was 1.9 - 2.1 x 10^{19} /m^3 in this case. The density was scanned from 1.0 to 2.5 x 10^{19} /m^3. The plasma current was also scanned from 50 to 80 kA. No major difference was found in the behavior of these parameters within this range. With the CCD camera, no arcing was observed without biasing. As seen in Fig. 1, the radiation loss P_{rad} and the intensity of MoI lines increased a little when the probe was inserted beyond 1.0 cm from the LCFS whereas the intensities of CIII and H_α unchanged. The absolute radiation loss was less than 40 kW, 30 - 40 % of the OH power throughout the discharge for the probe location r > 17 cm. Oxygen radiation OII increased in the first few shots after the insertion, then gradually decreased shot by shot, finally came back to the initial level before the insertion. Increase in Z_{eff} can be seen in Fig. 1. But the cause of this increase is unclear because the OII radiation was measured only in a toroidal section in the vicinity of the probe. Dominant contribution to Z_{eff} both with and without the probe insertion could come from oxygen because neither boronization nor titanium gettering was applied before this experiment.

With the insertion beyond 3.0 cm from the LCFS, increase in P_{rad} and decrease in T_{e0} was observed at this density after the flat-top. The typical time behavior of T_{e0} and P_{rad} this case is shown in Fig. 2. The total radiation loss increased significantly from 20 ms and reached as high as 110 kW, which was comparable to the OH power. A hollow T_e profile was seen in this case. With

further insertion beyond 4.0 cm, the plasma suffered from disruption due to strong interaction with the probe.

3.2. Probe biasing

For better understanding of the impurity generation mechanism at the surface and local transport in edge plasmas, both positive and negative bias were applied to the probe. The biasing voltage V_b was scanned between -100 and +100 volt.

Figure 3 shows time behavior of T_{e0} after the flat-top. The temperature T_{e0} was kept constant with the probe location at 18 cm without biasing and with positive biasing. On the contrary, negative biasing caused decrease in T_{e0} during the bias voltage. The radiation loss reached to the input power, which was responsible to this temperature collapse. The temperature showed recovery a little bit after the biasing was switched off. The CCD camera observation often indicated that arcing happened for voltages V_b between -80 and -100 volt. However the behavior in Fig. 3 was seen either with arcing or without arcing, and direct impact of the arcing was not clearly seen here. The radiation CIII increased by a factor 2 during the biasing whereas those of MoI, OII, H_α did not show significant change. A spike in the CIII intensities corresponded to arcing, too. Thus the negative biasing had an clear impact upon only the carbon radiation within the experimental observation until now.

Figure 4 shows edge plasma parameters with and without the biasing. Electron temperature rose by 10 eV both with negative and positive biasing, which could give a minor effect on the impact energy of ions to the surface. Sheath potential in front of the probe surface could give the dominant impact upon the energy of ions to the surface.

The penetration length of Mo neutrals was investigated with the CCD camera for these operations corresponding to Fig. 4. It was 1.9 mm without biasing, where the density at the LCFS was 2.3×10^{18} /m^3 . It was reduced to 1.2 mm with the positively biased discharge, where the density was 3.6×10^{18} /m^3. The gyration radius of a Mo^+ ion of 4 eV is 2.6 mm, which is larger than the decay lengths above shown. Probability of Mo ions penetration to the core might be smaller in these two cases than the negatively biased case. Nevertheless, it is not clear whether this difference is enough to explain the difference in plasma behavior in the negatively biased case.

It is hard to conclude which mechanism is responsible to the temperature collapse seen in Figs. 2 and 3. It is not likely the radiation loss due to the Mo impurities within this experimental observation, but is possibly relating to the enhanced carbon release from the Mo probe surface. Another possible cause might be change in transport in the core plasma with the biasing because all the parameters in front of the surface did not show significant change with the negative biasing except the CIII radiation.

3.3. Edge ohmic heating (EOH) discharges

A good confinement scheme of H-mode has been achieved in HT-6M by applying the edge ohmic heating (EOH) [10]. An additional voltage was applied to the plasma loop inductively, which raise the plasma current up to a new steady state with a ramp rate of 12 MA/s. After a few ms of this voltage spike, the plasma fell into the H-phase, which was characterized by a sudden drop in H_α signals. Energy confinement time increased by a factor 1.5, central density by a factor 1.3, and edge density by a factor 2, namely the density profile in the core became flat. Instability of m=2 was suppressed during the H-phase. A steep density gradient was formed in the region between r/a = 0.8 and 0.95. Density in SOL was lower, and temperature higher in the H-phase than those in L-phase. The H-mode threshold behavior has been investigated by scanning surface safety factor q_a and the additional OH power.

Figure 5 shows a diagram of L- and H- discharges as a function of the safety factor q_a and the OH power at the instant of applying the EOH voltage. The triangles in the diagram correspond to L-mode discharge without H-transition. The open triangles are those without the Mo probe (the probe being outside the LCFS) and the closed triangles with the Mo probe at 18.0 cm (1.5 cm inside the LCFS). The circles correspond to the discharges with the H-transition. Between the area of open triangles and of open circles, a clear border can be found between L- and H-discharges without the Mo probe as shown by a dashed line. Similar comparison in the case with the probe results in a new border shown by a solid line. This result indicates that the insertion of Mo probe causes the increase in the threshold power of L-H transition with the EOH.

Now we try to give an explanation to this result. In the H-phase, the pressure barrier is formed in the region from 0.8a to 0.95a. This region corresponds to r=15.6 cm and to 18.6 cm. When the probe was located at r > 18.5 cm, the probe was outside this region, which did not give significant impact upon the L-H transition behavior. Because of the short penetration length of Mo impurity from the probe surface, the influence of the probe could be localized to its vicinity. On the contrary, when the probe was at 18.0 cm, it was located already inside the barrier region, which could give a strong impact in this region.

As a conclusion, the experimental results suggest a certain operation range of the H-mode in the EOH discharge in HT-6M. However, this is still preliminary and a local result in HT-6M. Much more investigation is necessary to get a view which can be extrapolate to H-modes in other big tokamaks.

4. Summary and Conclusion

The Mo and W probe has been tested in HT-6M tokamak, and preliminary results for the Mo probe is presented.

(1) In normal OH discharges, the degradation of core plasma performance was found only when the probe was inserted beyond 3.0 cm inside the LCFS with the plasma density range between 1.0 - 2.5 x 10^{19} /m^3 . No significant change was seen up to 2.0 cm inside the LCFS.
(2) The plasma performance did not change with positive biasing to the probe. On the contrary, central T_e degraded during negative biasing of -100 V. Only the intensity of CIII increased in front of the probe surface. The mechanism which is responsible to this degradation is unclear within this experimental results.
(3) The insertion of the Mo probe to 1.5 cm inside the LCFS made a change in the threshold power of the L-H transition in EOH discharges. The result suggest a certain operation range of the H-mode in the EOH discharge with the Mo probe in HT-6M.

Acknowledgments

The authors are grateful to Drs. K. Adati and T. Watari for giving this opportunity of the collaboration work. This work was financially supported partly by Japanese Ministry of Education, Science and Culture through the Grant-in Aid for Scientific Research of No. 05044115 and No. 05045024.

References

[1] T. Tanabe, N. Noda, H. Nakamura, J. Nucl. Mater. 196-1988 (1992) 11.
[2] N. Noda, V. Philipps, R. Neu, this conference.
[3] V. Philipps, T. Tanabe, Y. Ueda et al., Nucl. Fusion 34 (1994) 1417.
[4] T. Tanabe, V. Philipps, Y. Ueda et al., J. Nucl. Mater. 212-215 (1994) 1370.
[5] Y. Ueda, T. Tanabe, V. Philipps et al., J. Nucl. Mater. 220-222 (1995) 240.
[6] D. Naujoks, K. Asmussen et al., Nucl. Fusion 36 (1996) 671.
[7] R. Neu et al., this conference.
[8] B. Lipschultz, J. Goetz, B. Labombard et al., J. Nucl. Mater. 220-222 (1995) 50.
[9] K. Ohasa, H. Maeda et al., Nucl. Fusion 18 (1978) 872.
[10] J. Li et al., in 15th IAEA Conf. in Sevilla, 1994 IAEA-CN 60/A2-II-2

Figure Captions

Fig. 1 Parameters measured as a function of the probe position r . Plasma current I_p was 66 kA, field strength B_T 1.0 T, T_{e0} 600 - 700 eV, average density n_e 1.9 - 2.1 x 10^{19} /m^3.

Fig. 2 Temporal behavior of the radiation loss P_{rad} and the central electron temperature T_{e0} with the Mo probe inserted to 3 cm inside the LCFS.

Fig. 3 Temporal behavior of the central electron temperature T_{e0} with the Mo probe inserted to 1.5 cm inside the LCFS, biased to ± 100 V. The signals at the same location without biasing and those without the Mo probe insertion are plotted as the reference.

Fig. 4 Edge density (a) and temperature (b) profiles for positive and negative biasing. The bias voltage Vb was applied from 25 ms to 55 ms.

Fig. 5 The diagram of L- and H-mode with the EOH discharges.
Open and closed triangles indicate L-mode discharges without and with the Mo probe, respectively. Open and closed circles indicate H-mode discharges without and with the Mo probe, respectively. A dashed line indicates the border between L- and H-mode region without the Mo probe, and a solid line that with the Mo probe (1.5 cm inside the LCFS).

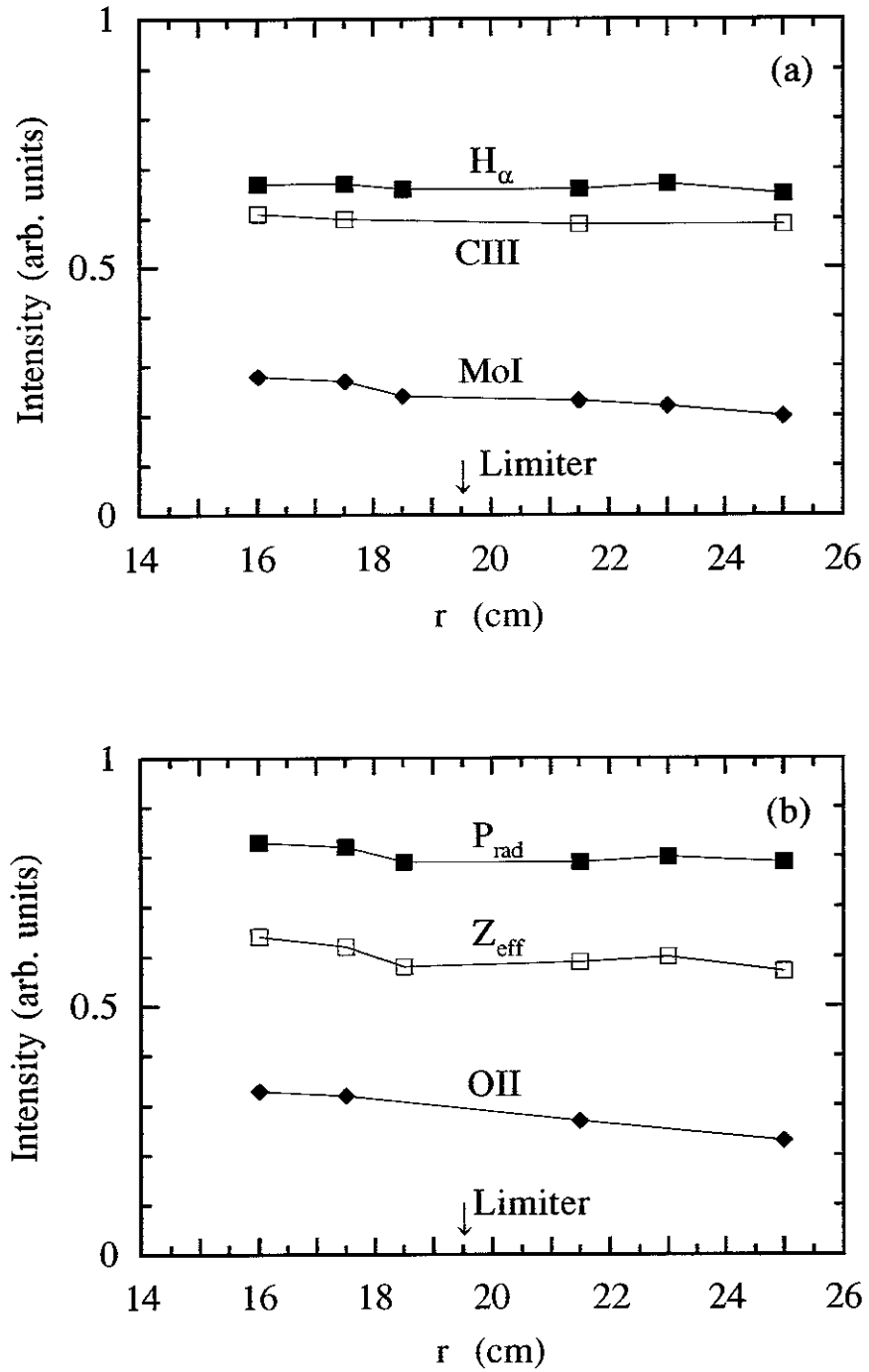

Fig. 1 Parameters measured as a function of the probe position r . Plasma current I_p was 66 kA, field strength B_T 1.0 T, T_{e0} 600 - 700 eV, average density n_e 1.9 - 2.1 x 10^{19} /m^3.

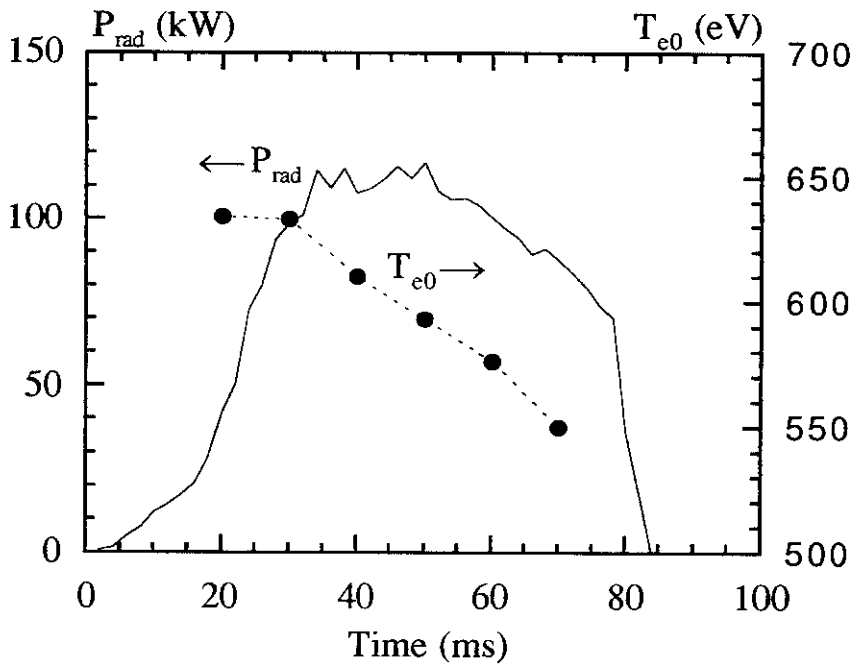

Fig. 2 Temporal behavior of the radiation loss P_{rad} and the central electron temperature T_{e0} with the Mo probe inserted to 3 cm inside the LCFS.

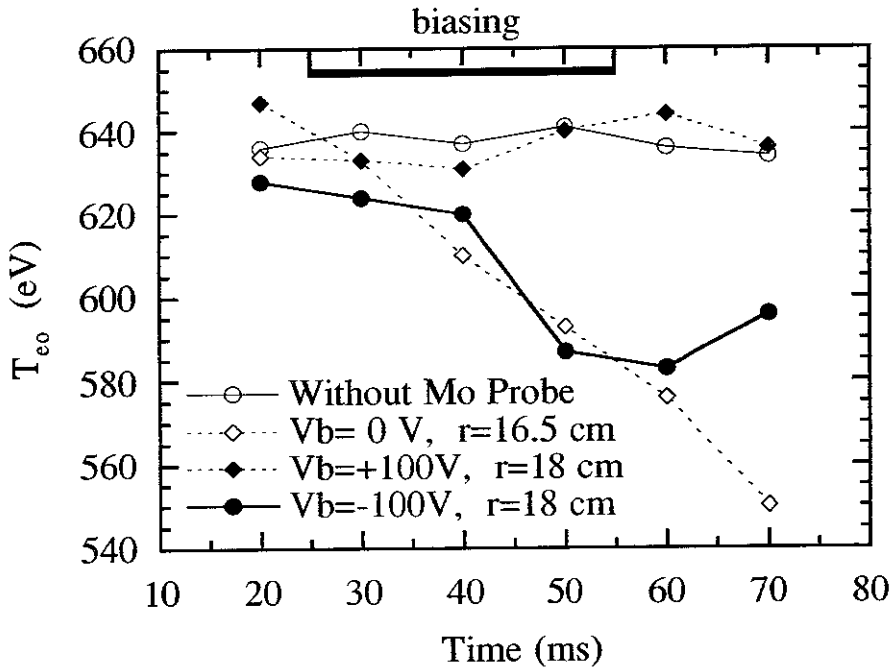

Fig. 3 Temporal behavior of the central electron temperature T_{e0} with the Mo probe inserted to 1.5 cm inside the LCFS, biased to ± 100 V. The signals at the same location without biasing and those without the Mo probe insertion are plotted as the reference.

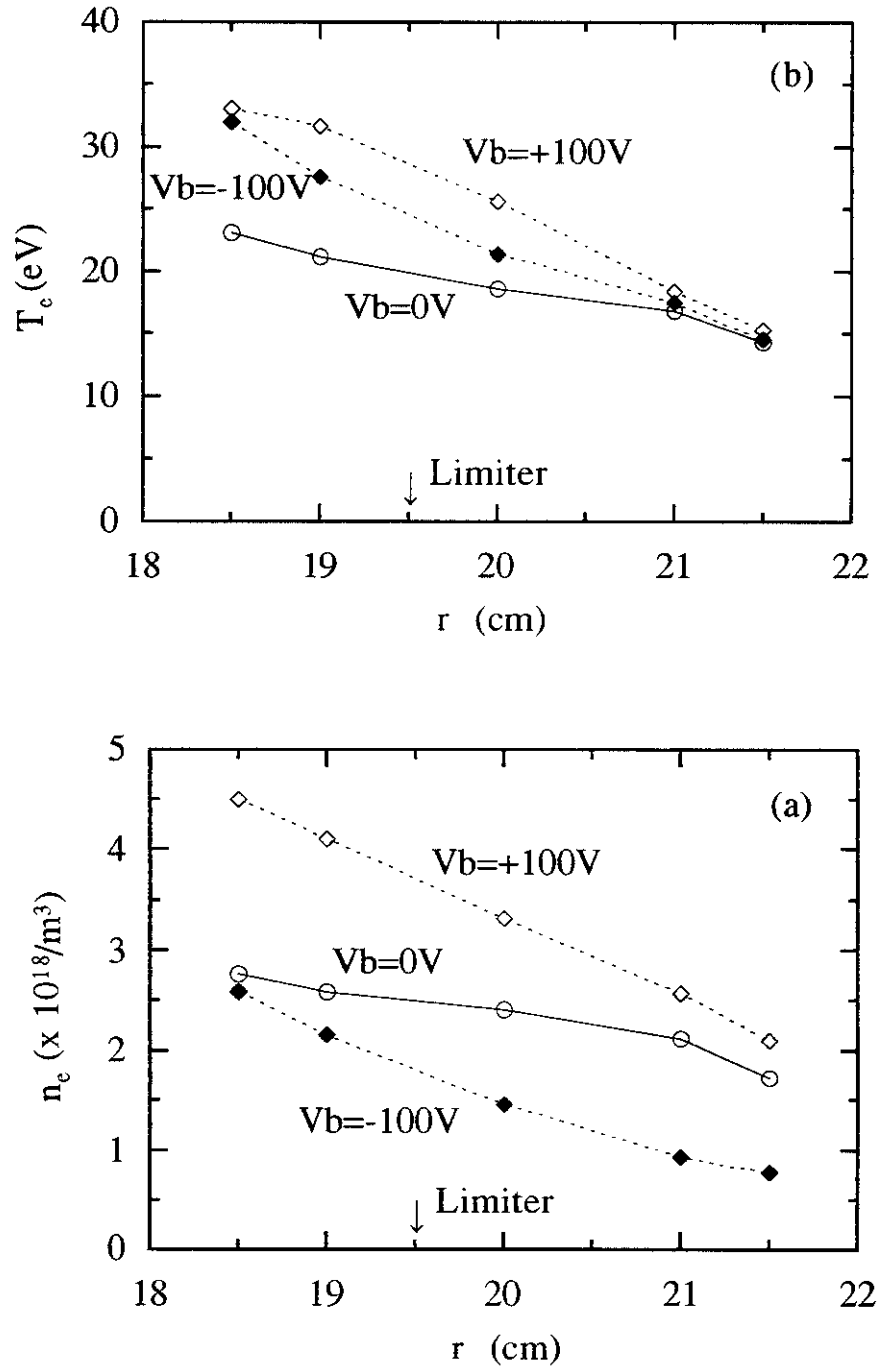

Fig. 4 Edge density (a) and temperature (b) profiles for positive and negative iasing. The bias voltage Vb was applied from 25 ms to 55 ms.

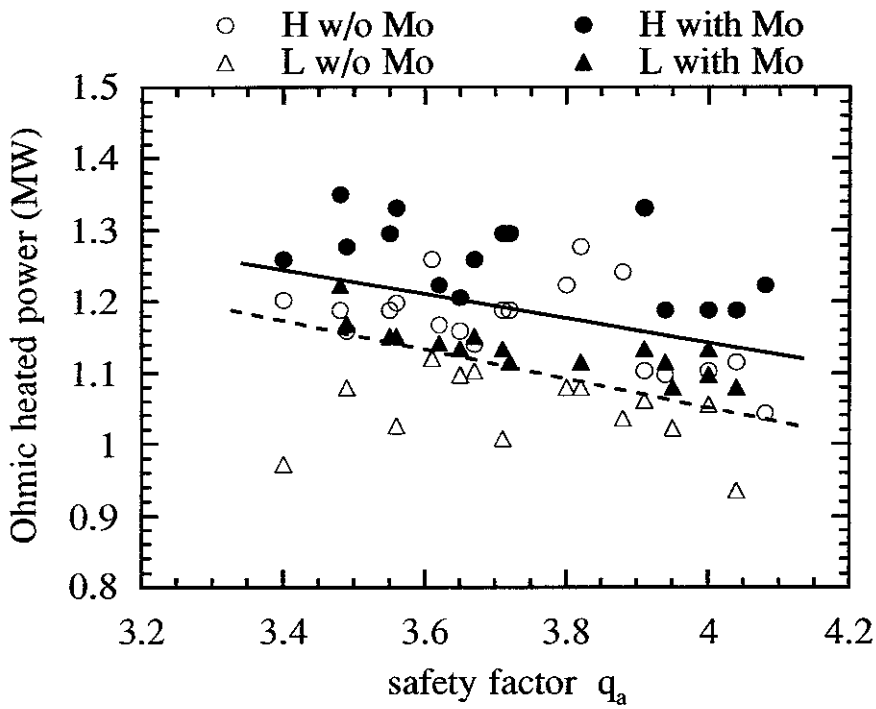

Fig. 5 The diagram of L- and H-mode with the EOH discharges.
Open and closed triangles indicate L-mode discharges without and with the Mo probe, respectively. Open and closed circles indicate H-mode discharges without and with the Mo probe, respectively. A dashed line indicates the border between L- and H-mode region without the Mo probe, and a solid line that with the Mo probe (1.5 cm inside the LCFS).

Recent Issues of NIFS Series

NIFS-415 A. Fujisawa, H. Iguchi, S. Lee, T.P. Crowley, Y. Hamada, S. Hidekuma, M. Kojima,
Active Trajectory Control for a Heavy Ion Beam Probe on the Compact Helical System; May 1996

NIFS-416 M. Iwase, K. Ohkubo, S. Kubo and H. Idei
Band Rejection Filter for Measurement of Electron Cyclotron Emission during Electron Cyclotron Heating; May 1996

NIFS-417 T. Yabe, H. Daido,T. Aoki, E. Matsunaga and K. Arisawa,
Anomalous Crater Formation in Pulsed-Laser-Illuminated Aluminum Slab and Debris Distribution; May 1996

NIFS-418 J. Uramoto,
Extraction of K^- Mesonlike Particles from a D_2 Gas Discharge Plasma in Magnetic Field; May 1996

NIFS-419 J. Xu, K. Toi, H. Kuramoto, A. Nishizawa, J. Fujita, A. Ejiri, K. Narihara, T. Seki, H. Sakakita, K. Kawahata, K. Ida, K. Adachi, R. Akiyama, Y. Hamada, S. Hirokura, Y. Kawasumi, M. Kojima, I. Nomura, S. Ohdachi, K.N. Sato
Measurement of Internal Magnetic Field with Motional Stark Polarimetry in Current Ramp-Up Experiments of JIPP T-IIU; June 1996

NIFS-420 Y.N. Nejoh,
Arbitrary Amplitude Ion-acoustic Waves in a Relativistic Electron-beam Plasma System; July 1996

NIFS-421 K. Kondo, K. Ida, C. Christou, V.Yu.Sergeev, K.V.Khlopenkov, S.Sudo, F. Sano, H. Zushi, T. Mizuuchi, S. Besshou, H. Okada, K. Nagasaki, K. Sakamoto, Y. Kurimoto, H. Funaba, T. Hamada, T. Kinoshita, S. Kado, Y. Kanda, T. Okamoto, M. Wakatani and T. Obiki,
Behavior of Pellet Injected Li Ions into Heliotron E Plasmas; July 1996

NIFS-422 Y. Kondoh, M. Yamaguchi and K. Yokozuka,
Simulations of Toroidal Current Drive without External Magnetic Helicity Injection; July 1996

NIFS-423 Joong-San Koog,
Development of an Imaging VUV Monochromator in Normal Incidence Region; July 1996

NIFS-424 K. Orito,
A New Technique Based on the Transformation of Variables for Nonlinear Drift and Rossby Vortices; July 1996

NIFS-425 A. Fujisawa, H. Iguchi, S. Lee, T.P. Crowley, Y. Hamada, H. Sanuki, K. Itoh, S. Kubo, H. Idei, T. Minami, K. Tanaka, K. Ida, S. Nishimura, S. Hidekuma, M. Kojima, C. Takahashi, S. Okamura and K. Matsuoka,
Direct Observation of Potential Profiles with a 200keV Heavy Ion Beam Probe and Evaluation of Loss Cone Structure in Toroidal Helical Plasmas on the Compact Helical System; July 1996

NIFS-426 H. Kitauchi, K. Araki and S. Kida,
Flow Structure of Thermal Convection in a Rotating Spherical Shell; July 1996

NIFS-427 S. Kida and S. Goto,
Lagrangian Direct-interaction Approximation for Homogeneous Isotropic Turbulence; July 1996

NIFS-428 V.Yu. Sergeev, K.V. Khlopenkov, B.V. Kuteev, S. Sudo, K. Kondo, F. Sano, H. Zushi, H. Okada, S. Besshou, T. Mizuuchi, K. Nagasaki, Y. Kurimoto and T. Obiki,
Recent Experiments on Li Pellet Injection into Heliotron E; Aug. 1996

NIFS-429 N. Noda, V. Philipps and R. Neu,
A Review of Recent Experiments on W and High Z Materials as Plasma-Facing Components in Magnetic Fusion Devices; Aug. 1996

NIFS-430 R.L. Tobler, A. Nishimura and J. Yamamoto,
Design-Relevant Mechanical Properties of 316-Type Stainless Steels for Superconducting Magnets; Aug. 1996

NIFS-431 K. Tsuzuki, M. Natsir, N. Inoue, A. Sagara, N. Noda, O. Motojima, T. Mochizuki, T. Hino and T. Yamashina,
Hydrogen Absorption Behavior into Boron Films by Glow Discharges in Hydrogen and Helium; Aug. 1996

NIFS-432 T.-H. Watanabe, T. Sato and T. Hayashi,
Magnetohydrodynamic Simulation on Co- and Counter-helicity Merging of Spheromaks and Driven Magnetic Reconnection; Aug. 1996

NIFS-433 R. Horiuchi and T. Sato,
Particle Simulation Study of Collisionless Driven Reconnection in a Sheared Magnetic Field; Aug. 1996

NIFS-434 Y. Suzuki, K. Kusano and K. Nishikawa,
Three-Dimensional Simulation Study of the Magnetohydrodynamic Relaxation Process in the Solar Corona. II.; Aug. 1996

NIFS-435 H. Sugama and W. Horton,
Transport Processes and Entropy Production in Toroidally Rotating Plasmas with Electrostatic Turbulence; Aug. 1996

NIFS-436 T. Kato, E. Rachlew-Källne, P. Hörling and K.-D Zastrow,
Observations and Modelling of Line Intensity Ratios of OV Multiplet Lines for 2s3s 3S1 - 2s3p 3Pj; Aug. 1996

NIFS-437 T. Morisaki, A. Komori, R. Akiyama, H. Idei, H. Iguchi, N. Inoue, Y. Kawai, S. Kubo, S. Masuzaki, K. Matsuoka, T. Minami, S. Morita, N. Noda, N. Ohyabu, S. Okamura, M. Osakabe, H. Suzuki, K. Tanaka, C. Takahashi, H. Yamada, I. Yamada and O. Motojima,
Experimental Study of Edge Plasma Structure in Various Discharges on Compact Helical System; Aug. 1996

NIFS-438 A. Komori, N. Ohyabu, S. Masuzaki, T. Morisaki, H. Suzuki, C. Takahashi, S. Sakakibara, K. Watanabe, T. Watanabe, T. Minami, S. Morita, K. Tanaka, S. Ohdachi, S. Kubo, N. Inoue, H. Yamada, K. Nishimura, S. Okamura, K. Matsuoka, O. Motojima, M. Fujiwara, A. Iiyoshi, C. C. Klepper, J.F. Lyon, A.C. England, D.E. Greenwood, D.K. Lee, D.R. Overbey, J.A. Rome, D.E. Schechter and C.T. Wilson,
Edge Plasma Control by a Local Island Divertor in the Compact Helical System; Sep. 1996 (IAEA-CN-64/C1-2)

NIFS-439 K. Ida, K. Kondo, K. Nagaski T. Hamada, H. Zushi, S. Hidekuma, F. Sano, T. Mizuuchi, H. Okada, S. Besshou, H. Funaba, Y. Kurimoto, K. Watanabe and T. Obiki,
Dynamics of Ion Temperature in Heliotron-E; Sep. 1996 (IAEA-CN-64/CP-5)

NIFS-440 S. Morita, H. Idei, H. Iguchi, S. Kubo, K. Matsuoka, T. Minami, S. Okamura, T. Ozaki, K. Tanaka, K. Toi, R. Akiyama, A. Ejiri, A. Fujisawa, M. Fujiwara, M. Goto, K. Ida, N. Inoue, A. Komori, R. Kumazawa, S. Masuzaki, T. Morisaki, S. Muto, K. Narihara, K. Nishimura, I. Nomura, S. Ohdachi, M.. Osakabe, A. Sagara, Y. Shirai, H. Suzuki, C. Takahashi, K. Tsumori, T. Watari, H. Yamada and I. Yamada,
A Study on Density Profile and Density Limit of NBI Plasmas in CHS; Sep. 1996 (IAEA-CN-64/CP-3)

NIFS-441 O. Kaneko, Y. Takeiri, K. Tsumori, Y. Oka, M. Osakabe, R. Akiyama, T. Kawamoto, E. Asano and T. Kuroda,
Development of Negative-Ion-Based Neutral Beam Injector for the Large Helical Device; Sep. 1996 (IAEA-CN-64/GP-9)

NIFS-442 K. Toi, K.N. Sato, Y. Hamada, S. Ohdachi, H. Sakakita, A. Nishizawa, A. Ejiri, K. Narihara, H. Kuramoto, Y. Kawasumi, S. Kubo, T. Seki, K. Kitachi, J. Xu, K. Ida, K. Kawahata, I. Nomura, K. Adachi, R. Akiyama, A. Fujisawa, J. Fujita, N. Hiraki, S. Hidekuma, S. Hirokura, H. Idei, T. Ido, H. Iguchi, K. Iwasaki, M. Isobe, O. Kaneko, Y. Kano, M. Kojima, J. Koog, R. Kumazawa, T. Kuroda, J. Li, R. Liang, T. Minami, S. Morita, K. Ohkubo, Y. Oka, S. Okajima, M. Osakabe, Y. Sakawa, M. Sasao, K. Sato, T. Shimpo, T. Shoji, H. Sugai, T. Watari, I. Yamada and K. Yamauti,
Studies of Perturbative Plasma Transport, Ice Pellet Ablation and Sawtooth

Phenomena in the JIPP T-IIU Tokamak; Sep. 1996 (IAEA-CN-64/A6-5)

NIFS-443 Y. Todo, T. Sato and The Complexity Simulation Group,
Vlasov-MHD and Particle-MHD Simulations of the Toroidal Alfvén Eigenmode; Sep. 1996 (IAEA-CN-64/D2-3)

NIFS-444 A. Fujisawa, S. Kubo, H. Iguchi, H. Idei, T. Minami, H. Sanuki, K. Itoh, S. Okamura, K. Matsuoka, K. Tanaka, S. Lee, M. Kojima, T.P. Crowley, Y. Hamada, M. Iwase, H. Nagasaki, H. Suzuki, N. Inoue, R. Akiyama, M. Osakabe, S. Morita, C. Takahashi, S. Muto, A. Ejiri, K. Ida, S. Nishimura, K. Narihara, I. Yamada, K. Toi, S. Ohdachi, T. Ozaki, A. Komori, K. Nishimura, S. Hidekuma, K. Ohkubo, D.A. Rasmussen, J.B. Wilgen, M. Murakami, T. Watari and M. Fujiwara,
An Experimental Study of Plasma Confinement and Heating Efficiency through the Potential Profile Measurements with a Heavy Ion Beam Probe in the Compact Helical System; Sep. 1996 (IAEA-CN-64/C1-5)

NIFS-445 O. Motojima, N. Yanagi, S. Imagawa, K. Takahata, S. Yamada, A. Iwamoto, H. Chikaraishi, S. Kitagawa, R. Maekawa. S. Masuzaki, T. Mito, T. Morisaki, A. Nishimura, S. Sakakibara, S. Satoh, T. Satow, H. Tamura, S. Tanahashi, K. Watanabe, S. Yamaguchi, J. Yamamoto, M.Fujiwara and A. Iiyoshi,
Superconducting Magnet Design and Construction of LHD; Sep. 1996 (IAEA-CN-64/G2-4)

NIFS-446 S. Murakami, N. Nakajima, S. Okamura, M. Okamoto and U. Gasparino,
Orbit Effects of Energetic Particles on the Reachable β–Value and the Radial Electric Field in NBI and ECR Heated Heliotron Plasmas; Sep. 1996 (IAEA-CN-64/CP -6) Sep. 1996

NIFS-447 K. Yamazaki, A. Sagara, O. Motojima, M. Fujiwara, T. Amano, H. Chikaraishi, S. Imagawa, T. Muroga, N. Noda, N. Ohyabu, T. Satow, J.F. Wang, K.Y. Watanabe, J. Yamamoto , H. Yamanishi, A. Kohyama, H. Matsui, O. Mitarai, T. Noda, A.A. Shishkin, S. Tanaka and T. Terai
Design Assessment of Heliotron Reactor; Sep. 1996 (IAEA-CN-64/G1-5)

NIFS-448 M. Ozaki, T. Sato and the Complexity Simulation Group,
Interactions of Convecting Magnetic Loops and Arcades; Sep. 1996

NIFS-449 T. Aoki,
Interpolated Differential Operator (IDO) Scheme for Solving Partial Differential Equations; Sep. 1996

NIFS-450 D. Biskamp and T. Sato,
Partial Reconnection in the Sawtooth Collapse; Sep. 1996

NIFS-451 J. Li, X. Gong, L. Luo, F.X. Yin, N. Noda, B. Wan, W. Xu, X. Gao, F. Yin, J.G. Jiang, Z. Wu., J.Y. Zhao, M. Wu, S. Liu and Y. Han,
Effects of High Z Probe on Plasma Behavior in HT-6M Tokamak; Sep. 1996